Structure Elucidation at the Nanomole Scale. 1. Trisoxazole Macrolides and Thiazole-Containing Cyclic Peptides from the Nudibranch *Hexabranchus sanguineus*

Doralyn S. Dalisay,[†] Evan W. Rogers,[†] Arthur S. Edison,[‡] and Tadeusz F. Molinski*[,†,§]

Department of Chemistry and Biochemistry and Skaggs School of Pharmacy and Pharmaceutical Sciences, MC0358, 9500 Gilman Drive, La Jolla, California 92093-0358, and National High Magnetic Field Laboratory and Department of Biochemistry & Molecular Biology, University of Florida, Gainesville, Florida 32610

Received December 1, 2008

A single specimen of *Hexabranchus sanguineus*, a nudibranch from the Indo-Pacific that is known to sequester kabiramides B and C and other trisoxazole macrolides, yielded new kabiramide analogues, 9-desmethylkbiramide B and 33-methyltetrahydrohalichondramide, and two new unexpected thiazole-containing cyclic peptides in submicromolar amounts. The structures of these cyclic peptides were determined by analyses of 1D and 2D NMR spectra recorded with a state-of-the-art 1 mm ^{1}H NMR high-temperature superconducting microcryoprobe, together with mass spectra. In addition to two proline residues, each peptide contains a thiazole- or oxazole-modified amino acid residue, together with conventional amino acid residues. All of the amino acid residues were L, as determined by Marfey's analysis of the acid hydrolysates of the peptides. This is the first report of cyclic thiazole peptides from *H. sanguineus.* Since thiazole-oxazole-modified peptides are typically associated with cyanobacteria and tunicates, the finding may imply a dietary component of the *H. sanguineus* that was previously overlooked.

The Indo-Pacific nudibranch *Hexabranchus sanguineus* (a shell-less opistobranch mollusk) and its egg masses contain extraordinary bioactive polyketide macrolide natural products known as "trisoxazole" macrolides. The three contiguous 2,4-disubstituted oxazole rings, which constitute the outstanding structural feature of trisoxazole macrolides, are integrated within a larger macrolide ring that is further appended by an aliphatic chain terminated by an *N*-methyl-*N*-vinylformamide. The first examples of trisoxazoles, ulapualides A and B[1] and kabiramide C (**1**), were reported in 1986;[2] however, a subsequent report described the related analogue halichondramide from the sponge *Halichondria* sp. collected in Palau.[3] At about the same time, dihydrohalichondramide and tetrahydrohalichondramide were found in specimens of *H. sanguineus*,[4] collected in Kwajalein atoll, and also in egg masses laid by live individuals in captivity. Like many dorid nudibranchs, *H. sanguineus* is a specialist predator with a spongiverous diet; in an aquarium, the nudibranch was found to consume only *Halichondria* containing trisoxazole macrolides and not sponges of other species or genera.[5] These observations provided strong evidence that *H. sanguineus* acquires its suite of trisoxazole compounds from a selective sponge diet and the first confirmatory evidence of the passage of trisoxazoles macrolides from sponge to nudibranch to progeny.

Trisoxazole macrolides exhibit extremely potent antifungal and cytotoxic activities, properties that appear to correlate with their tight binding to G-actin, depolymerization of F-actin, and disruption of actin filament formation and organization.[6] Finally, trisoxazoles are concentrated in tissue of *Hexabranchus* at levels higher than those found in the sponge and provide the animal with a potent chemical defense against crustaceans and fish. For example, the common Pacific wrasse *Thalasomma lunare* was deterred from consuming krill pellets that were treated with trisoxazoles at concentrations as low as 10 ppm.[5]

Since 1986, over two dozen analogues, including kabiramide B (**2**),[7] have been described from *H. sanguineus*[8] and other sponges of the genera *Jaspis*,[9] *Mycale*,[10] and *Pachastrissa.*[11] Our own investigations of the extract from a single specimen of *H. sanguineus* collected in Fiji uncovered **1**[2] and **2**[7] as the major antifungal metabolites; however at that time NMR instrumentation was insufficient to allow investigation of the minor constituents and the extract fractions were archived (−20 °C) for almost two decades. In 2007−2008, we gained access to two 600 MHz NMR spectrometers with highly sensitive probes, a custom-built 1 mm high-temperature superconducting (HTS) NMR cryoprobe[12] (National High Magnetic Field Laboratory) and a commercial 1.7 mm cryoprobe, which allowed full characterization of the very minor components of *H. sanguineus*. The HTS cryoprobe was constructed with four Helmholtz pairs (^{1}H, ^{2}H, ^{13}C, and ^{15}N) of planar sapphire supporting plates that were coated with a thin film of YBCO (yttrium−barium−copper oxide). The HTS coils and conventional cryoprobe preamplifier components are cooled to 20 K using a commercial cryogenic cooling system.[12] The combination of high intrinsic coil sensitivity, low noise, and very small fill volume (∼5−10 μL) give ^{1}H NMR spectra with exceptional mass sensitivity and opens investigations of new natural products with complex structures from rare sources where only as little as a few nanomoles may be available.[13] In this report, we describe our application of the microcryoprobes with unmatched sensitivity to elucidate the structures of the very minor natural products from a single specimen of *H. sanguineus:* two new trisoxazole analogues, 9-*O*-desmethyl kabiramide B (**3**) and 33-methyltetrahydrohalichondramide (**5**), together with two unexpected thiazole-containing peptides, which we named sanguinamides A (**7**) and B (**8**). These complex structures were fully characterized from submicromole samples by 1D and 2D ^{1}H and ^{13}C NMR data together with MS and degradative correlation.

Results and Discussion

A single specimen of *H. sanguineus* was collected by hand in Fiji (1987) in the Yasawa Island chain. The deep-red acetone extract of *H. sanguineus* was partitioned between ethyl acetate and water. The ethyl acetate-soluble portion was fractionated by silica chromatography followed by C_{18} reversed-phase chromatography to give the new compounds 9-*O*-desmethylkabiramide B (**3**, 0.04% w/w dry weight), 33-methyltetrahydrohalichondramide (**5**, 0.07%), and sanguinamides A (**7**, 0.023%) and B (**8**, 0.011%) in addition to the known compounds **1** (2.2%),[2] **2**[7] (0.12%), kabiramide D[7] (0.24%), and 33-methyldihydrohalichondramide[7] (0.28%).

* To whom correspondence should be addressed. Tel: +1 (858) 551-1662. Fax: +1 (858) 822-0386. E-mail: tmolinski@ucsd.edu.
† Department of Chemistry and Biochemistry, UC San Diego.
§ Skaggs School of Pharmacy and Pharmaceutical Sciences, UC San Diego.
‡ University of Florida.

10.1021/np8007649 CCC: $40.75
Published on Web 03/02/2009

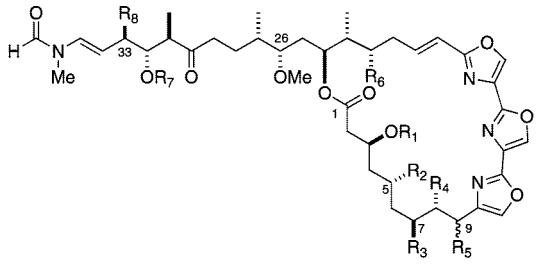

	R_1	R_2	R_3	R_4	R_5	R_6	R_7	R_8
1	$CONH_2$	Me	OH	Me	α-OMe	OMe	Me	Me
2	$CONH_2$	Me	OH	Me	α-OMe	OH	Me	Me
3	$CONH_2$	Me	OH	Me	α-OH	OH	Me	Me
4	H	H	OH	Me	β-OMe	H	Me	H
5	H	H	OH	Me	β-OMe	H	Me	Me
6	H	OH	=O	Me	β-OMe	H	Me	H

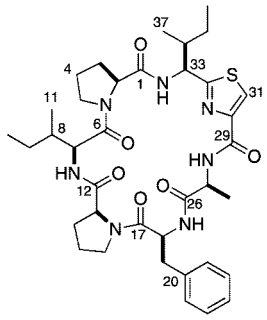

7

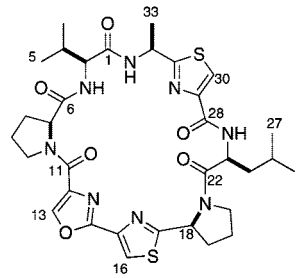

8

Compound **3** was shown to be the homologue of **2** with the formula $C_{46}H_{67}N_5O_{14}Na$ established by HRESIMS (*m/z* 936.4574, $[M + Na]^+$) and most likely arises from loss of a *C*-methyl or an *O*-methyl group. As with all trisoxazoles, the NMR spectra were observed as slowly interconverting rotamers (∼2:1) due to restricted rotation about the *N*-methyl−formamide bond. The ^1H NMR spectrum of **3** was similar to that of **2** except only two OMe singlets (δ 3.28, s; 3.29, s) were present instead of three. The COSY, HMBC, and HSQC data indicated that **3** had the same carbon framework as **2** including the characteristic ^1H NMR singlets for the three oxazole rings (δ 7.72, s, H-11; 8.32, s H-14; 8.27, s, H-17). Since **2** has OMe groups at C-9, C-26, and C-32, one of these must be replaced by an OH group in **3**. The HMBC and HSQC data for **3** showed that the position of the new OH group was at C-9 because the two OMe signals (δ 3.28, s; 3.29, s) were located unambiguously at C-26 (δ 56.8, q) and C-32 (δ 60.3, q) through long-range correlations. The remaining ^1H NMR signals of **3** were essentially identical to those of **2**.

Compound **5** has a molecular formula of $C_{45}H_{67}N_4O_{12}$ as determined by HRESIMS (*m/z* 855.4738 $[M + H]^+$) with one CH_2 unit more than tetrahydrohalichondramide (**4**).[4] The ^1H NMR data of **5** revealed five *C*-methyl signals (δ 1.02, d, $J = 6.8$ Hz; 0.87, d, $J = 7.2$ Hz; 0.84, d, $J = 7.2$ Hz; 0.92, d, $J = 6.8$ Hz and 1.16, d, $J = 6.8$ Hz) corresponding to C-8-Me, C-23-Me, C-27-Me, C-31-Me, and C-33-Me, respectively. The ^1H NMR signal due to H-33 in **5** appeared as a multiplet (δ 2.38, m) and corresponds to replacement by CH for the two diastereotopic CH_2 signals in **4** (δ 2.50, m, 1H; 2.17, m, 1H). Careful analysis of COSY and TOCSY spectra revealed correlations of the C-33-Me signal (δ 1.16, d, $J =$ 6.8 Hz) to H-32, H-33, H-34, and H-35 and located the additional *C*-methyl group at C-33. Thus, **5** has the structure 33-methyltetrahydrohalichondramide.

The absolute configurations of **3** and **5** were assigned by comparisons to the trisoxazoles kabiramide C (**1**) and jaspisamide A (**6**) and deductions based on conformational analysis and $^1H-^1H$ *J* coupling. The absolute configurations of several of the trisoxazoles have been assigned by separate groups using different approaches. Panek and co-workers assigned mycalolide A by degradation, synthesis of degradation products, and, ultimately, the natural product.[14] None of the trisoxazole macrolides have delivered crystals suitable for X-ray analysis; however the excellent work of Rayment and co-workers provided unambiguous absolute configurations for trisoxazoles by separate single-crystal X-ray analyses[6] of G-actin bound with **1**, jaspisamide A (**6**),[9] halichondramide,[4,5] and ulapualide.[15b] Not only did this reveal the relationship of the latter natural products to the marine-derived macrolides reidispongiolides and sphinxolides,[14] but this milestone work served to remove stereochemical ambiguities and corrected[15b] an anomalous assignment[16] of at least one trisoxazole macrolide based on the "facts and fantasies"[17] of untested metal-chelation hypotheses.[18]

The C-9 configuration changes in different trisoxazoles[6] and the C-9-OMe substitutent may be α or β; however the configurations of other methyl-branched stereocenters in trisoxazole families appear to be invariant. For reasons of optimum deuterium-lock strength, the ^1H NMR spectra of **3** were recorded in CD_3CN (600 MHz, 1 mm HTS probe); however NMR data for other trisoxazoles[8] have been mostly reported in $CDCl_3$. Comparisons based on chemical shift alone may compromise arguments for the C-9 relative configuration in **3**. For example, the polar H-bond acceptor solvent CD_3CN may coordinate the free OH groups and influence the local conformation and electronic environment around the 1,3-diol moiety and chemical shifts with respect to **2**. In order to resolve this problem, we examined the Rayment X-ray structures[6] of jaspisamide A (**6**) and kabiramide C (**1**), which share similar C-6−C-9 segments but have epimeric C-9 configurations. Although both X-ray structures were determined for G-actin-bound trisoxazoles, the macrolide ring segments show minimal contacts to protein residues and their conformations are likely to be similar to the solution structures. The ring conformations of **1** and **6** (Figure 1) are remarkably similar; the three contiguous oxazole rings form a planar wall, tilted approximately at an angle of ∼22° to the averaged macrolide ring plane defined by the ester C=O group and the extended (zigzag) C-2−C-9 chain. In both molecules, the C-7−O bond of the oxygen substituent (OH in **1** and C=O in **6**) points *endo* to the macrolide ring, and the C-8−Me bond is perpendicular to the average macrolide plane. The major difference between the two molecules is the orientation of the C-9 OMe group. In jaspisamide A (**6**), the β-OMe group lies pseudoequatorial, almost in-plane with the macrolide ring, but in kabiramide C (**1**), C-9 has the epimeric configuration with a pseudoaxial α-OMe substitutent almost *anti* to the C-8 methyl group. The corresponding dihedral angles H-8−C-8−C-9−H-9 for **1** and **6** are −78° and +68°, respectively, and give rise to an H-9 ^1H NMR signal that is a broad singlet (δ 5.19, bs) for **1** and a doublet for **6** (δ 4.98, d, $J = 4.4$ Hz).[9] Since the vicinal coupling constant between H-8 and H-9 in **3** is very small ($J \approx 0$ Hz), this compound must have the same C-9 α-OMe configuration found in **1**. Using similar arguments, the *J* values and chemical shifts of **4** and **5** were found to be similar to those of halichondramide,[3,4] and we tentatively assigned the C-9 β-OMe configuration to **5**, as depicted here.

Further examination of the minor components of *H. sanguineus* gave, unexpectedly, two new peptides, **7** and **8**. Sanguinamide A (**7**) was isolated as a minor component from a fraction containing the trisoxazole compounds. HRESIMS gave the formula $C_{37}H_{52}N_7O_6S$ (*m/z* 722.3683 $[M + H]^+$) with 16 degrees of unsaturation. The ^1H NMR data of **7** revealed signals typical of a peptide: four amide NH proton signals (Table 1, δ 9.19, d, $J = 7.2$ Hz; 8.78, d, $J = 7.2$ Hz; 8.11, d, $J = 7.8$ Hz; 6.11, bs) and six α-CH signals (δ 3.38 d, $J = 7.6$ Hz, H-13; 4.22, ddd, $J = 10.1$, 5.8, 1.7 Hz, H-18; 4.26, dd, $J = 10.0$, 7.2 Hz, H-7; 4.67, d, $J =$ 7.9 Hz, H-2; 4.69, qd, $J = 7.8$, 6.4 Hz, H-27; 5.09, t, $J = 7.2$ Hz, H-33). HSQC showed a downfield broad ^1H singlet (δ 8.01, s, H-31)

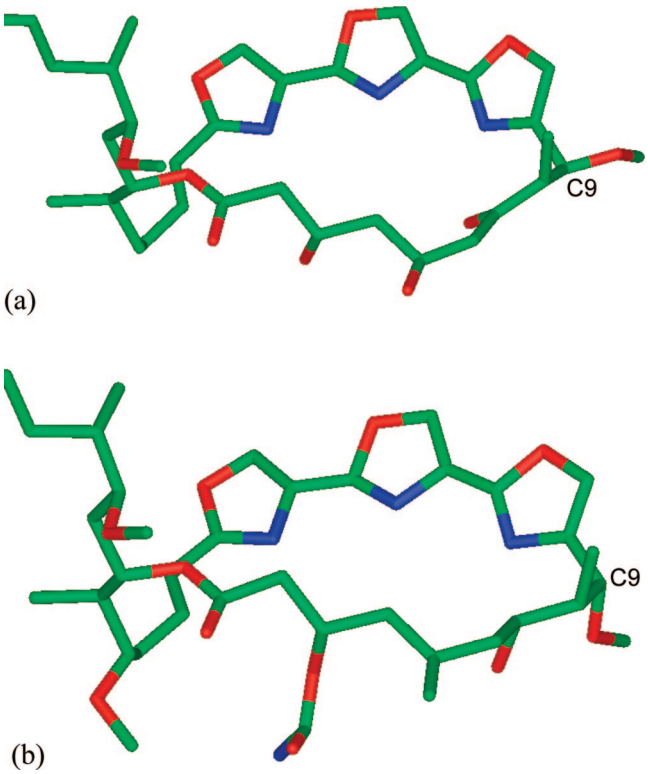

Figure 1. X-ray structures of trisoxazoles bound to G-actin (data adapted from Rayment et al., ref 6): (a) jaspisamide A (**6**), torsional angles C-8(Me)−C-8−C-9−C-10 = −57.4°, H-8−C-8−C-9−H-9 = +67.9°; (b) kabiramide C (**1**), torsional angles C-8(Me)−C-8−C-9−C-10 = −67.3°, H-8−C-8−C-9−H-9 = +75.8°. Side chains of each compound (upper left) and protein residues have been removed for clarity.

coupled to a ^{13}C signal (δ 123.1, d, C-31) characteristic of C-4 in a 2-substituted thiazole-4-carboxamide. This was verified by HMBC data, which showed correlations from H-31 to other thiazole ring carbon signals at δ 148.5, 160.3, and 168.1.

The identities of six remaining amino acid residues—two Pro, two Ile, Ala, and Phe—were revealed by analysis of COSY, TOCSY, HSQC, and HMBC data (Table 1). Therefore, sanguinamide A (**7**) is a modified heptapeptide. The amino acid sequence of **7** was defined from the HMBC correlations between the α-CH and amide-NH proton signals with the adjacent C═O group. An HMBC correlation was observed from the α-CH of Pro-1 (H-2) and the C═O of Ile-1 (δ 174.5, s, C-6). The amide-NH proton of Ile-1 (δ 9.19) showed a correlation to C═O of Pro-2 (δ 171.5, s, C-12). In turn, the α-proton of Pro-2 (H-13) showed a cross-peak to the C═O of Phe (δ 169.2, s, C-17), and the α-CH signal of Phe (H-18) showed connectivity to the C═O group of Ala (δ 171.0, s, C-26).

The above HMBC correlations provided the partial structure Pro1-Ile1-Pro2-Phe-Ala, which was connected to the thiazole-modified amino acid as follows. The H-31 singlet showed an HMBC correlation to the Thz C═O (δ 160.3, s, C-29), which in turn was correlated to ^1H NMR signals of the Ala α-CH (H-27) and NH (δ 8.11). The last residue, Ile-2, identified through COSY correlations, constitutes the thiazole-modified amino acid residue. Mutual correlations (Figure 2a) were observed from the Ile-2 NH (δ 8.78), α-CH (H-33), and H-31 signals to the thiazole carbon C-32 (δ 168.1, s). Finally, an HMBC correlation between the amide proton at δ 8.78 and α-CH signal (H-33) of Ile2-thiazole fragment and C═O of Pro-1 (δ 170.6, s, C-1) returns to the first residue, closes the ring, and completes the structure of cyclic peptide **7**.

Sanguinamide B (**8**), $C_{33}H_{43}N_8O_6S_2$ (HRESIMS *m/z* 711.2723 $[M + H]^+$), is a larger peptide than **7** with 17 degrees of unsaturation. The ^1H NMR features of **8** are indicative of differences in amino acid composition from **7**, in particular the presence of three azole-modified amino acids instead of one. The backbone ^1H NMR signals included three amide-NH protons, confirmed by MS deuterium exchange (δ 9.60, d, J = 7.2 Hz; 9.26, d, J = 6.6 Hz; 8.42, d, J = 6.6 Hz), and five α-CH proton resonances (δ 4.39, d, J = 6.6 Hz, H-7; 4.61, d, J = 6.0 Hz, H-2; 5.29, dd, J = 16.8, 7.8 Hz, H-23; 5.56, dq, J = 7.2, 6.6, Hz, H-32). Evidence for the presence of three five-membered ring heterocycles include three downfield ^1H NMR singlets (δ 7.95, s, H-16; 8.12, s, H-30; 8.27, s, H-13), which were coupled (HSQC) to their respective ^{13}C nuclei (δ 121.8, d, C-16; 124.1 d, C-30; 141.5 d, C-13), accounting for two thiazoles and one 2-substituted oxazole 4-carboxamide. Long-range H−H couplings from the two broad singlets H-16 and H-30 to those ^{13}C signals in the two thiazole rings (Table 2) were identified as before with **7**; however the third singlet, H-13, showed long-range couplings to carbon signals that were significantly shifted

Table 1. NMR Data of Sanguinamide A,**7** (600 MHz, $CDCl_3$)

#	δ_C[a], mult.	δ_H, mult. (J in Hz)	HMBC
		L-Pro-1	
1	170.6, qC		
2	60.8, CH	4.67, d (7.9)	1, 6
3	30.5, CH_2	1.81, m	1, 4, 5
		2.68, dd (12.0, 5.2)	
4	25.0, CH_2	1.90, 2.02, m	2
5	48.1, CH_2	3.67, 4.00, m	4
		L-Ile-1	
6	174.5, qC		
7	56.3, CH	4.26, dd (10.0, 7.2)	6, 8, 9, 12
8	35.5, CH	2.30, m	
9	25.3, CH_2	1.24, 1.70, m	8, 10
10	15.1, CH_3	1.02, d (6.8)	7, 8, 9
11	10.3, CH_3	0.91, t (7.6)	8, 9
NH		9.19, d (7.2)	12
		L-Pro-2	
12	171.50, qC		
13	60.9, CH	3.38, d (7.6)	12, 17
14	30.4, CH_2	0.93, m	12, 16
		2.10, dd (12.2, 6.1)	
15	22.0, CH_2	1.70, 1.50, m	13
16	46.3, CH_2	3.50, 3.53, m	15
		L-Phe	
17	169.2, qC		
18	54.5, CH	4.22, ddd (10.1, 5.8, 1.7)	19, 26
19	37.9, CH_2	2.98, dd (11.9, 5.8)	17
		3.08, dd (11.9, 11.9)	
20	134.3, qC		
21	129.3, CH	7.16, d (7.10)	20, 22, 23
22	127.8, CH	7.24, m	
23	129.1, CH	7.28, m	
NH		6.11, br s	
		L-Ala	
26	171.0, qC		
27	49.1, CH	4.69, qd (7.8, 6.4)	26, 28, 29
28	17.9, CH_3	1.48, d (6.4)	26, 27
NH		8.11, d (7.8)	26, 29
		Thz	
29	160.3, qC		
30	148.5, qC		
31	123.1, CH	8.01, s	29, 30, 32
32	168.1, qC		
		L-Ile-2	
33	56.3, CH	5.09, dd (7.2, 7.2)	1, 32, 34, 35
34	40.9, CH	1.80, m	35
35	25.9, CH_2	1.17, 1.50, m	34, 36
36	15.0, CH_3	0.77, d (6.7)	33, 34, 35
37	10.3, CH_3	0.91, t (7.6)	34, 35
NH		8.78, d (7.2)	1, 32

[a] δ's measured by indirect detection, HSQC, and HMBC ($^1J_{CH}$ = 6 Hz). [b] $^1H \rightarrow ^{13}C$.

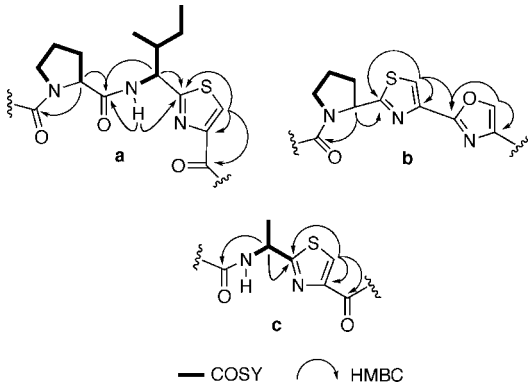

Figure 2. Subunits of sanguinamide A (**7**, a) and sanguinamide B (**8**, b,c), showing ^{1}H−^{1}H COSY and HMBC correlations.

Table 2. ^{1}H and ^{13}C NMR Data of Sanguinamide B, **8** (600 MHz, $CDCl_3$)

#	δ_C[a], mult.	δ_H, mult. (J in Hz)	HMBC[b]
		L-Val	
1	159.1, qC		
2	58.7, CH	4.61, d (6.0)	1
3	30.6, CH	2.93, m	
4	20.4, CH_3	0.87, d (6.6)	
5	20.2, CH_3	1.15, d (6.6)	
−NH		9.26, d (6.6)	2, 3, 6
		L-Pro-1	
6	170.4, qC		
7	60.9, CH	4.39, d (6.6)	6, 11
8	29.4, CH_2	1.74, 2.80, m	6
9	25.2, CH_2	2.22, 1.94, m	
10	45.4, CH_2	3.75, 3.34, m	
		Oxz	
11	169.2, qC		
12	136.7, qC		
13	141.5, CH	8.27, s	12, 14
14	157.7, qC		
		Thz-1	
15	142.3, qC		
16	121.8, CH	7.95, s	14, 15, 17
17	172.9, qC		
		L-Pro-2	
18	58.7, CH	4.57, d (6.0)	17, 22
19	31.1, CH_2	2.94, 2.07, m	17
20	28.7, CH_2	2.10, 1.81, m	
21	48.0, CH_2	3.81, 3.97, m	
		L-Leu	
22	170.8, qC		
23	48.4, CH	5.29, dd (16.8, 7.8)	22, 28
24	41.4, CH	2.02, m	
25	25.6, CH_2	1.63, m	
26	23.2, CH_3	0.99, d (6.6)	
27	22.0, CH_3	1.03, d (6.7)	
−NH		9.60, d (7.2)	
		Thz-2	
28	160.1, qC		
29	149.2, qC		
30	124.1, CH	8.12, s	28, 29, 31
31	170.6, qC		
		L-Ala	
32	47.8, CH	5.56, qd (7.2 6.6)	1, 31
33	24.8, CH_3	1.68, d (6.6)	31
−NH		8.42, d (7.2)	1, 31

[a] δ's measured by indirect detection, HSQC, and HMBC ($^1J_{CH}$ = 6 Hz). [b] ^{1}H→^{13}C.

downfield (δ 136.7, C-12; 157.7, C-14), indicative of oxazole. Spin systems for five additional amino acid residues—two Pro, Val, Leu, and Ala—were identified by ^{1}H NMR, COSY, and TOCSY experiments, and the sequence was solved as before using HMBC correlations of the α-CH and −NH resonances to the adjacent C═O ^{13}C signals. The −NH of Val (δ 9.26) was correlated to the C═O of Pro-1 (δ 170.4, s, C-6), and the α-CH of Pro-1 (H-7) was correlated to the C═O of the oxazole-4-carboxamide (δ 169.2, s, C-11). The H-16 signal showed an HMBC correlation to heterocyclic ^{13}C nuclei (δ 157.7, C-14; 142.3, C-15; 172.9, C-17), indicating that the oxazole and thiazole rings in **8** were connected to each other as shown (Figure 2b). Extending the sequence, the α-CH of Pro-2 (H-18) was correlated with C-17 (δ 172.9, s), showing that four of the five cyclic amino acid residues were contiguous.

Completion of the sequence was done by correlating the α-CH of Pro-2 (H-18) to the C═O of Leu and the α-CH of Leu to the C═O of the Thz-2 ring. The thiazole-modified amino acid Ala-Thz (Thz-1) was established by identifying correlations from α-CH (H-32), NH, and β-Me (δ 1.68, d, J = 6.4 Hz) to ^{13}C resonances within the heterocyclic ring and C-31 (δ 170.6, Figure 2c), as with **7**. Finally, the macrolactam ring of the octapeptide **8** was completed by connecting the Ala α-CH (H-32) and the amide proton (δ 8.42, d) to the C═O signal of Val (δ 159.1, s, C-1).

Rotation about tertiary proline amide bonds is restricted, and, in peptides, the Pro residue may adopt either *s-trans* or *s-cis* conformations. The *syn* β-CH_2 group is shielded by the C═O group in *s-cis* Pro residues with respect to the γ-CH_2 group; therefore the difference in ^{13}C chemical shifts between the C_β and C_γ signals in Pro amino acid residues ($\Delta\delta_{\beta\gamma} = \delta_\beta - \delta_\gamma$) in peptides is diagnostic of *s-cis* and *s-trans* conformations of the Pro amide bond; *s-cis* Pro residues have a larger difference than *s-trans* Pro residues.[19] The $\Delta\delta_{\beta\gamma}$ values measured for Pro-1 and Pro-2 in the heptapeptide **7** (5.5 and 8.4 ppm, respectively) indicate the *s-cis* conformation for both residues. In contrast, the more flexible octapeptide **8** has smaller $\Delta\delta_{\beta\gamma}$'s for Pro-1 (4.2 ppm) and Pro-2 (2.4 ppm), which is consequently assigned the *s-trans* configuration at each residue.

The absolute configuration of both **7** and **8** was determined by total hydrolysis of the peptides followed Marfey's analysis.[20] Given the known propensity for racemization at α-CH centers of thiazole-modified peptides, samples of **7** and **8** were split into two pools; one of which was first subjected to ozonolysis prior to total hydrolysis (6 M HCl, 110 °C, 16 h) to degrade the heterocyclic rings. The limited supply of **7** and **8** precluded the standard Marfey's method[20] and required optimized derivatization followed by sub-nanomole detection of the each amino acid derivative using ultrahigh-pressure liquid chromatography−mass spectrometry (UPLC-MS) and single-ion monitoring (SIM). These criteria were fulfilled, and complete configurational analysis was achieved on ∼30−50 μg of each peptide; all the amino acid residues in **7** and **8** were found to have the L-configuration.

Some comment is in order with respect to the absolute mass sensitivity of a 600 MHz spectrometer equipped with a 1 mm HTS cryoprobe (measurement of compounds **3** and **5**) or a commercial 1.7 mm cryoprobe (compounds **7** and **8**). Both probes have the significant advantage of cryocooled (∼20 K) preamplifier and probe components and fill volumes far smaller than conventional 5 mm ^{1}H inverse-detect cryoprobes (∼600 μL). Mass sensitivity is inversely proportional to the diameter of the coil, but this increased mass sensitivity comes at a cost of reduced volume. The smaller diameter of the HTS 1 mm probe, with a fill volume of ∼5−7 μL, provides high mass sensitivity but also requires a relatively high sample concentration. The mass sensitivity of the two probes can be compared from S/N values of 0.1% ethylbenzene/$CDCl_3$: 292:1 and 1120:1 for the 1 and 1.7 mm probes, respectively. When normalizing for the total volume of the sample, the 1 mm HTS probe has a *slightly* higher mass sensitivity than the 1.7 mm cryoprobe: 292/7 μL ≈ 42 μL^{-1} versus 1120/30 μL ≈ 37 μL^{-1}. Thus, there is a slight mass sensitivity advantage for the 1 mm probe, but the larger volume of the 1.7 mm probe provides greater

Table 3. Minimum Inhibitory Activity, MIC (μg/mL), of Trisoxazole Macrolides against Pathogenic *Candida* and *Cryptococcus neoformans* Strains (positive control, amphotericin B, AMB)

	Candida albicans ATCC 14503	*C. glabrata*	*C. neoformans* var. *grubii*
1	0.016	0.25	0.125
2	0.50	0.50	1.00
3	2.00	1.00	2.00
5	0.250	0.125	0.50
AMB	0.016	0.25	0.016

overall sensitivity and can be used to study less concentrated samples. In practice both probes gave exceptionally high *mass sensitivity* for compounds of relatively high MW and a large number of resonances. Perhaps more significant is the fact that complete NMR data sets of submicromolar amounts of molecules **3**, **5**, **7**, and **8** (C_{37}−C_{45})—greater in complexity than the majority of submicromolar natural products measured with capillary or microprobes[21,13]—were easily obtained in time frames similar to those encountered in conventional NMR. Clearly, this portends success for natural products discovery that previously was unattainable, particularly applications in characterization of novel drug leads from rare marine organisms.[22]

The antifungal mechanism of action of trisoxazole macrolides is likely related to tight binding to G-actin, depolymerization of F-actin, and disruption of actin filament formation and organization.[6] Compounds **1**−**3** and **5** and the clinical antifungal agent amphotericin B (AMB) were assayed for antifungal activity against *Candida* sp. and *Cryptococcus neoformans* (Table 3). Compound **1** showed the most potency against all fungal strains tested with an MIC nearly equal to the AMB. Compound **3** was least inhibitory against the strains of *Candida* and *Cryptococcus*.

Two new antifungal trisoxazole macrolides, **3** and **5**, were isolated from *H. sanguineus* in addition to two unexpected cyclic peptides, **7** and **8**. The structures of all four compounds were solved by MS and NMR, aided by data collected on extremely mass-sensitive NMR cryo-microprobes with limited materials at the nanomole scale. Cyclic peptides **7** and **8** have not been found in sponges consumed by *H. sanguineus*, suggesting either a different as-yet unidentified dietary source or *de novo* biosynthesis.

Experimental Section

General Experimental Procedures. All solvents for HPLC purification were HPLC grade. CD spectra were recorded on a Jasco J810 spectropolarimeter in 0.2 cm quartz cells at 23 °C unless otherwise stated. UV−vis spectra were recorded in a dual-beam Jasco V630 spectrometer in 1 cm quartz cells. ^{1}H and ^{13}C NMR spectra were recorded in $CDCl_3$ using either a Varian Mercury-400 (400 MHz), Varian Unity-500 (500 MHz), Bruker DMX-600 (600 MHz) equipped with a 1.7 mm {^{13}C}^{1}H CPTCI probe, or a custom built high-temperature superconducting probe (1 mm {^{13}C,^{15}N}^{1}H HTS, 600 MHz; design and performance features of this probe are described elsewhere).[12] NMR spectra were measured in $CDCl_3$ and referenced to residual solvent signals (^{1}H, δ 7.26 ppm; ^{13}C, δ 77.16 ppm). HRMS measurements were measured at The Scripps Research Institute (TOF-MS) or University of California, San Diego (EI-MS) mass spectrometry facilities. IR spectra were recorded on thin films using a Jasco 4100 FTIR and attenuated total reflectance (ATR, 3 mm ZnSe) plate. LCMS was carried out on a ThermoFisher Accela UPLC coupled to an MSQ single quadrupole mass spectrometer operating in positive ion mode, unless otherwise stated. Semipreparative HPLC was carried out on a Varian SD200 system equipped with a dual-pump and UV-1 UV detector under specified conditions.

Extraction and Isolation. The nudibranch *Hexabranchus sanguineus* was collected in the Yasawa Islands, Fiji, in 1987. The sample (N = 1) was immediately frozen and stored at −20 °C until extraction (~12 months). Frozen tissue was thawed and extracted with acetone (2 times), and each acetone extract was filtered and concentrated before partitioning between EtOAc and water. The EtOAc layers were concentrated under reduced pressure to give a dark orange oil. The second batch of acetone extract was separated by silica chromatography using a shallow gradient (1% MeOH/CH_2Cl_2, 2% MeOH/CH_2Cl_2, 4% MeOH/CH_2Cl_2 and 50% MeOH/CH_2Cl_2), giving six fractions. Fraction 90.001.6 was purified twice by reversed-phase HPLC (Dynamax, 5 μm, C_{18} column, 10 × 250 mm, 80:20 MeOH/H_2O, 3.5 mL/min, and (Dynamax, 5 μm, C_{18} column, 4.6 × 250 mm, 80:20 MeOH/H_2O, 1.5 mL/min), yielding 620 μg of pure **2** (t_R = 12.10 min). Fraction 90.001.5 was separated under reversed-phase HPLC (Dynamax semiprep, 25 × 1 cm; 83:17 MeOH/H_2O, 3.5 mL/min) to obtain three fractions. Fraction 90.001.5A was purified by reversed-phase HPLC (Zorbax Agilent, 5 μm, C_{18} column, 4.6 × 250 mm, 50:50 CH_3CN/H_2O), yielding two major fractions of **1** (16.64 mg) and crude **4**. Final purification by reversed-phase HPLC (Phenylhexyl Luna, 4.6 × 250 mm, 50:50 CH_3CN/H_2O, 1 mL/min, detection at 230 nm) yielded **3** (620 μg, t_R = 15.2 min), additional **1** (5.64 mg, t_R = 16.40 min), and pure **4** (1.30 mg, t_R = 21.04 min). Fraction 90.001.5B was further purified by reversed-phase HPLC (Phenylhexyl Luna, 4.6 × 250 mm, 50:50 CH_3CN/H_2O, 1.5 mL/min) to provide **8** (190 μg, t_R = 11.0 min), **7** (390 μg, t_R = 12.30 min), and **5** (1.3 mg, t_R = 18.0 min).

9-*O*-Desmethyl kabiramide B (3): colorless film; UV (MeOH) λ_{max} (log ε) 243 nm (4.38); IR (ATR) ν 3200−3600 br, 1618 cm^{-1}; ^{1}H NMR (600 MHz, CD_3CN, 1 mm HTS probe) δ 8.36 (0.7H, s, H-42), 8.32 (1H, s, H-14), 8.27 (1H, s, H-17), 8.04 (0.3H, s, H-42), 7.72 (1H, s, H-11), 7.25 (1H, ddd, J = 14.0, 8.5, 5.8 Hz, H-20), 7.07 (0.3H, d, J = 14.0 Hz, H-35), 6.39 (1H, d, J = 14.0 Hz, H-19), 6.62 (0.7H, d, J = 14.0 Hz, H-35), 5.19 (1H, br s, H-9), 5.15 (1H, m, H-3), 5.16 (0.3H, d, J = 14.0 Hz, H-34), 5.08 (0.7H, d, J = 14.0 Hz, H-34), 5.07 (1H, dd, J = 10.7, 7.0 Hz, H-24), 3.99 (1H, m, H-22), 3.92 (1H, br s, H-7), 3.84 (1H, br s, C-9-OH), 3.50 (1H, br s, C-7-OH), 3.36 (1H, d, J = 6.0 Hz, C-22-OH), 3.29 (3H, s, C-32-MeO), 3.28 (3H, s, C-26-OMe), 3.27 (1H, m, H-32), 3.09 (3H, m, C-35-NMe), 3.06 (1H, m, H-26), 2.74 (1H, dd, J = 7.2, 6.5 Hz, H-31), 2.58 (0.3H, m, H-33), 2.52 (1H, m, H-29′), 2.51 (1H, m, H-21′), 2.50 (1H, m, H-29), 2.50 (1H, m, H-2′), 2.45 (0.7H, m, H-33), 2.31 (1H, m, H-21), 2.30 (1H, m, H-2), 2.15 (1H, dd J = 8.0, 7.0 Hz, H-8), 1.81 (1H, m, H-5), 1.81 (1H, m, H-6), 1.81 (1H, m, H-6′), 1.72 (1H, m, H-27), 1.71 (1H, m, H-28), 1.65 (1H, m, H-23), 1.64 (1H, m, H-25′), 1.58 (1H, m, H-4′), 1.50 (1H, m, H-25), 1.31 (1H, m, H-4), 1.22 (1H, m, H-28′), 1.36 (3H, d, J = 7.0 Hz, H-41), 0.95 (3H, d, J = 7.0 Hz, H-36), 0.91 (3H, d, J = 7.0 Hz, H-40), 0.90 (3H, d, J = 7.0 Hz, H-38), 0.87 (3H, d, J = 8.0 Hz, H-37), 0.82 (3H, d, J = 7.0 Hz, H-39); ^{13}C NMR (indirect detection, HSQC, and HMBC (J_{CH} = 6 Hz), 600 MHz) δ 214.1 (C, C-30), 175.8 (C, C-1), 163.5 (NHCHO), 145.4 (CH, C-20), 138.3 (CH, C-17), 137.9 (CH, C-14), 136.9 (C, C-10), 135.9 (CH, C-11), 131.4 (C, C-13), 130.7 (C, C-16), 111.4 (113.7*) (CH, C-34), 88.4 (89.6*) (CH, C-32), 82.02 (CH, C-26), 74.5 (CH, C-24), 74.0 (CH, C-9), 69.5 (CH, C-22), 68.7 (CH, C-7), 67.6 (CH, C-3), 60.3 (C-32-OMe), 56.8 (C-26-OMe), 49.7 (CH, C-31), 45.1 (CH_2, C-4), 43.1 (CH_2, C-6), 42.9 (CH, C-23), 41.3 (CH_2, C-29), 41.2 (CH_2, C-2), 38.3 (CH, C-8), 38.1 (38.0*) (CH, C-33), 36.1 (CH_2, C-21), 35.0 (CH, C-27), 33.7 (CH_2, C-25), 27.7 (NMe), 26.5 (CH, C-5), 25.6 (CH_2, C-28), 18.3 (19.3*) (CH_3, C-41), 18.1 (CH_3, C-36), 15.7 (CH_3, C-40), 15.5 (CH_3, C-39), 9.5 (CH_3, C-38) (*minor isomer); HREIMS m/z 936.4574 [M + Na]$^+$ (calcd for $C_{46}H_{67}N_5O_{14}Na$, 936.4582).

33-Methyl tetrahydrohalichondramide (5): colorless film; UV (MeOH) λ_{max} (log ε) 233 nm (4.53); IR (ATR) ν 3200−3600 br, 1584 cm^{-1}; ^{1}H NMR 600 MHz ($CDCl_3$) δ 8.28 (0.7H, s, H-41), 8.10 (1H, s, H-17), 8.07 (0.3H, s, H-41), 8.05 (1H, m, H-14), 7.63 (1H, s, H-11), 7.13 (0.3H, d, J = 14.0 Hz, H-35), 6.99 (1H, dt, J = 16.0, 8.0 Hz, H-20), 6.46 (1H, d, J = 0.7 Hz, H-35), 6.43 (1H, d, J = 16.0 Hz, H-19), 5.20 (1H, m, H-24), 5.09 (1H, m, H-34), 4.39 (1H, d, J = 3.0 Hz, H-9), 4.22 (1H, m, H-3), 3.93 (1H, m, H-7), 3.30 (1H, m, H-32), 3.50 (3H, s, C-9-OMe), 3.35 (3H, s, C-26-OMe), 3.34 (3H, s, C-32-OMe), 3.04 (3H, s, NMe), 2.97 (1H, br d, J = 10.0 Hz, H-26), 2.64 (1H, dq, J = 9.0, 7.0 Hz, H-31), 2.69 (1H, m, H-6), 2.67 (1H, m, H-6′), 2.53 (1H, m, H-2), 2.48 (1H, m, H-21), 2.48 (2H, m, H-29), 2.43 (1H, br qd, J = 7.0, 4.5 Hz, H-8), 2.38 (1H, m, H-33), 2.26 (1H, m, H-21′), 1.85 (2H, m, H-5), 1.79 (1H, m, H-28′), 1.77 (2H, m, H-23), 1.71 (2H, m, H-27), 1.71 (1H, m, H-4), 1.71 (1H, m, H-22′), 1.61 (1H, m, H-4′), 1.56 (1H, m, H-25), 1.34 (1H, m, H-22′), 1.16 (3H, d, J = 7.0 Hz, H-40), 1.02 (3H, d, J = 7.0 Hz, H-36), 0.92 (3H, d, J = 7.0 Hz, H-39), 0.87 (3H, d, J = 7.0 Hz, H-37), 0.84 (3H, d, J = 7.0 Hz, H-38); ^{13}C NMR (indirect detection, HSQC, and HMBC (J_{CH} = 8 Hz), 600 MHz) δ 213.6 (C, C-30), 173.2 (C, C-1), 162.1(160.8*) (NHCHO), 162.0

(C, C-18), 156.3 (C, C-15), 155.0 (C, C-12), 143.2 (CH, C-20), 141.3 (C, C-10), 137.7 (CH, C-17), 137.4 (CH, C-14), 136.7 (CH, C-11), 130.9 (C, C-13), 129.9 (124.6*) (CH, C-35), 129.7 (C, C-16), 116.3 (CH, C-19), 111.0 (113.0*) (CH, C-34), 82.4 (CH, C-32), 82.4 (CH, C-9), 81.9 (CH, C-26), 73.9 (CH, C-24), 71.0 (CH, C-7), 68.7 (CH, C-3), 61.2 (C-9-OMe), 58.9 (C-26-OMe), 57.9 (C-32-OMe), 48.9 (CH, C-31), 42.5 (CH_2, C-2), 42.1 (CH_2, C-29), 38.8 (CH, C-8), 37.6 (CH, C-33), 36.7 (CH_2, C-4), 35.7 (CH, C-23), 34.7 (CH, C-27), 33.3 (CH_2, C-6), 32.1 (CH_2, C-25), 31.5 (CH_2, C-22), 28.8 (CH_2, C-21), 27.6 (33.4*) (NMe), 25.3 (CH_2, C-28), 22.4 (CH_2, C-5), 19.4 (CH_3, C-40), 15.6 (CH_3, C-38), 13.7 (CH_3, C-37), 13.3 (CH_3, C-39), 9.1 (CH_3, C-36) (*minor isomer); HREIMS *m/z* 855.4738 $[M + H]^+$ (calcd for $C_{45}H_{67}N_4O_{12}$, 855.4750).

Sanguinamide A (7): colorless film; IR (ATR) ν 2922, 2852, 1733, 1646, 1541 cm^{-1}; CD (MeOH) λ_{max} ($\Delta\varepsilon$) 224 nm (−14.5); ^1H (600 MHz, 1.7 mm probe) and ^{13}C NMR, see Table 1; HREIMS *m/z* 722.3683 $[M + H]^+$ (calcd for $C_{37}H_{52}N_7O_6S$, 722.3694)

Sanguinamide B (8): colorless film; UV (MeOH) λ_{max} (log ε) 250 nm (4.7); IR (ATR) ν 2980, 2357, 1589 cm^{-1}; CD (MeOH) λ_{max} ($\Delta\varepsilon$) 235 nm (−4.30); ^1H (600 MHz, 1.7 mm probe) and ^{13}C NMR, see Table 2; HREIMS *m/z* 711.2723 $[M + H]^+$ (calcd for $C_{33}H_{43}N_8O_6S_2$, 711.2723).

Determination of Absolute Configuration of 7 and 8. (a) Ozonolysis and Hydrolysis of Peptides. Samples of peptide were split into two pools, A and B. The first pool (A) was ozonolyzed prior to hydrolysis as follows: **7** (50 μg) and **8** (30 μg) were individually suspended in ozone-saturated MeOH (150 μL) at −78 °C for 5 min before concentration of the solvent under a N_2 stream at −78 °C to remove ozone, then to dryness at 0 °C. Pool B samples, **7** (50 μg), **8** (30 μg), and ozonolyzed samples from pool A were each individually resuspended in degassed, freshly distilled constant-boiling 6 N HCl (200 μL) and heated in a flame-sealed glass tube at 110 °C for 15 h. The mixtures were concentrated to dryness under a stream of N_2 and redissolved in 100 μL of H_2O.

(b) Marfey's Derivatization with L-FDLA. [20] Each of the above hydrolysates was treated with a solution of 2,4-dinitrophenyl-5-fluoro-L-leucinamide (100 μL, 1% w/v in acetone), followed by 1.0 M $NaHCO_3$ (25 μL), then heated in a sealed tube at 80 °C for 10 min. The mixture was cooled and quenched with 1.0 M HCl (25 μL). Authentic L- and D-amino acid standards were treated under identical conditions.

(c) LC-MS Analysis. The Marfey's derivatives (see above) were analyzed by LC-MS using a ThermoElectron Accela series ultrahigh-pressure liquid chromatograph (UPLC) with a Thermo Hypersil Gold C-18 column (50 mm × 2.1 mm, 1.9 μm) or Agilent Zorbax SB-Aq C18 column (250 mm × 4.6 mm, 5 μm) connected to a PDA and ThermoFinnigan MSQ quadrapole mass spectrometer. LC parameters were as follows: Hypersil: flow rate 0.5 mL/min, initial 80% solvent A (H_2O + 0.1% formic acid), 20% solvent B (acetonitrile), hold 0.3 min, at 9 min 40% A, at 10 min 100% B hold for 3 min, at 14 min 80% A hold for 2 min; Zorbax SB-Aq: flow rate 1.0 mL/min, initial 95% solvent A (H_2O + 0.1% formic acid) 5% solvent B (acetonitrile), hold 2 min, at 65 min 40% A, at 67 min 100% B hold for 5 min, at 73 min 95% A hold for 5 min. Injection volume was 3 μL. PDA parameters were as follows: channel A 340 nm, channel B 254 nm. MSQ parameters were as follows: ESI-MS, selected ion monitoring at *m/z* 384.15, 410.17, 412.18, 426.20, 460.18 $[M + H]^+$, span 1.5 amu, dwell 0.6 s, cone 75 V, probe temperature 450 °C. Retention times for the amino acids on the Hypersil in min t_R= (L/D) were as follows: alanine (4.28/5.16), proline (4.32/4.99), valine (5.07/6.61), phenylalanine (5.85/7.12), *allo*-isoleucine (5.64/7.26), isoleucine (5.67/7.36), leucine (5.75/7.39). Because of overlap of peaks of the *allo*-isoleucine and isoleucine FDLA derivatives on the C_{18} Hypersil column, these substituted amino acids were analyzed on the Zorbax SB-Aq column, which gave the following retention times: *allo*-isoleucine (55.79/62.38), isoleucine (56.17/62.42). Co-injections of L-*allo*-isoleucine and L-isoleucine FDLA derivatives with the corresponding derivatives from **7** and **8** were used to verify the assignments.

In Vitro Antifungal Testing. The fungal isolates used in this study were strains of *Candida albicans* (2 clinical isolates that are fluconazole-resistant, strain UCDFR1 and 96-489, and a reference strain, ATCC 14503) and clinical isolates of *Candida glabrata*, *Candida krusei*, *Cryptococcus neoformans* var. *grubii*, and *C. neoformans* var. *gattii*. The fungi were grown and maintained in Sabouraud dextrose agar, SDA plates (BBL, 211584), and incubated at 30 °C for 24 h (*Candida* sp.) or 48 h (*C. neoformans*). The *in vitro* susceptibility of each compound was determined by the broth microdilution method according to the guidelines of the National Committee for Clinical Laboratory Standards (NCCLS).[23] Briefly, 2-fold serial dilutions of compounds were prepared in 96-well microtiter plates (Corning Incorporated, 3595) from stock solutions in an RPMI-1640 broth medium (Sigma) buffered to a final pH of 7.0 with 0.165 M morpholinepropanesulfonic acid (MOPS; Sigma) to a final volume of 100 μL. A stock solution was prepared in dimethyl sulfoxide (DMSO, Sigma) for the various compounds and for amphotericin B, AMB (Sigma), which was used as positive control. The final drug concentrations tested were from 0.062 to 64 μg/mL and from 0.0078 to 8 μg/mL for amphotericin B. All fungal strains were tested in replicate in each run of the experiments. Cell growth was determined by the OD at 600 nm using a Spectramax Plus 384 microplate reader (Molecular Devices, CA). The MIC end point was defined as the lowest concentration with complete (≥90%) growth inhibition.

Acknowledgment. We are grateful to T. M. Zabriskie (Oregon State University) for collection of *H. sanguineus*, C. M. Ireland (University of Utah) for expedition logistics, T. Kühn (Bruker, Switzerland) for some of the 1.7 mm cryoprobe NMR data, and Brandon I. Morinaka for helpful discussions. We thank J. Pawlik (University of North Carolina, Wilmington) for the image of *H. sanguineus* (graphic abstract). Mass spectra were provided by Scripps Research Institute MS Facility and Y. Su (UCSD MS Facility). This research was supported by grants from the NIH (RO1 AI 039987, CA122256 to T.F.M.) and National High Magnetic Field Laboratory support (to A.S.E.). The 1 mm HTS instrument time was provided by the NSF-funded NHMFL external user program.

Supporting Information Available: ^1H NMR, 2D NMR, and CD spectra of **3**, **5**, **7**, and **8**. This material is available free of charge via the Internet at http://pubs.acs.org.

References and Notes

(1) Roesener, J. A.; Scheuer, P. J. *J. Am. Chem. Soc.* **1986**, *108*, 846–847.
(2) Matsunaga, S.; Fusetani, N.; Hashimoto, K.; Koseki, K.; Noma, M. *J. Am. Chem. Soc.* **1986**, *108*, 847–849.
(3) (a) Kernan, M. R.; Faulkner, D. J. *Tetrahedron Lett.* **1987**, *28*, 2809–2812. (b) Kernan, M. R. Ph.D. Thesis, University of California, San Diego, 1988.
(4) Kernan, M. R.; Molinski, T. F.; Faulkner, D. J. *J. Org. Chem.* **1988**, *53*, 5014–5020.
(5) Pawlik, J. R.; Kernan, M. K.; Molinski, T. F.; Harper, M. K.; Faulkner, D. J. *J. Exp. Mar. Biol. Ecol.* **1988**, *119*, 99–109.
(6) Klenchin, V. A.; Allingham, J. S.; King, R.; Tanaka, J.; Marriott, G.; Rayment, I. *Nat. Struct. Biol.* **2003**, *10*, 1058–1063.
(7) Matsunaga, S.; Fusetani, N.; Hashimoto, K.; Koseki, K.; Noma, M.; Noguchi, H.; Sankawa, U. *J. Org. Chem.* **1989**, *54*, 1360–1363.
(8) Matsunaga, S. *Prog. Mol. Subcell. Biol.* **2006**, *43*, 241–60.
(9) Kobayashi, J.; Murata, O.; Shigemori, H.; Sasaki, T. *J. Nat. Prod.* **1993**, *56*, 787–91.
(10) Fusetani, N.; Yasumuro, K.; Matsunaga, S.; Hashimoto, K. *Tetrahedron Lett.* **1989**, *30*, 2809–2812.
(11) Petchprayoon, C.; Asato, Y.; Higa, T.; Garcia-Fernandez, L. F.; Pedpradab, S.; Marriott, G.; Suwanborirux, K.; Tanaka, J. *Heterocycles* **2006**, *69*, 447.
(12) Brey, W. W.; Edison, A. S.; Nast, R. E.; Rocca, J. R.; Saha, S.; Withers, R. S. *J. Magn. Reson.* **2006**, *179*, 290–293.
(13) Molinski, T. F. *Curr. Opin. Drug Discovery Dev.* **2009**, in press.
(14) Matsunaga, S.; Liu, P.; Celatka, C. A.; Panek, J. S.; Fusetani, N. *J. Am. Chem. Soc.* **1999**, *121*, 5605−5606 [*corr.*; Matsunaga, S.; Liu, P.; Celatka, C. A.; Panek, J. S.; Fusetani, N. *J. Am. Chem. Soc*. **1999**, *121*, 8969].
(15) (a) Allingham, J. S.; Zampella, A.; D'Auria, M. V.; Rayment, I. *Proc. Natl. Acad. Sci. U.S.A.* **2005**, *102*, 14527–14532. (b) Allingham, J. S.; Tanaka, J.; Marriott, G.; Rayment, I. *Org. Lett.* **2004**, *6*, 597–599.
(16) Chattopadhyay, S. K.; Pattenden, G. *Tetrahedron Lett.* **1998**, 6095–6098.
(17) Michael, J. P.; Pattenden, G. *Angew. Chem., Intl. Ed.* **1993**, *32*, 1–130.
(18) Maddock, J.; Pattenden, G.; Wight, P. G. *Comput.-Aided Mol. Des.* **1993**, *7*, 573–585. In fact, experimental evidence based on fluorescence measurements suggests that trisoxazole macrolides *do not chelate* divalent metal ions and, with the exception of Hg^{2+}, ligate poorly with

common row 2 transition metal ions. James, D. M.; Wintner, E.; Faulkner, D. J.; Siegel, J. S. *Heterocycles* **1993**, *35*, 675–678.
(19) (a) Dorman, D. E.; Bovey, F. A. *J. Org. Chem.* **1973**, *38*, 2379–2383, and references within. (b) Siemion, I. Z.; Wieland, T.; Pook, K. *Angew. Chem., Int. Ed.* **1975**, *14*, 702–703.
(20) Marfey, P. *Carlsberg. Res. Commun.* **1984**, *49*, 591–596.
(21) Schroeder, F. C.; Gronquist, M. *Angew. Chem., Int. Ed.* **2006**, *45*, 7122–7131.
(22) Molinski, T. F.; Dalisay, D. S.; Lievens, S. L.; Saludes, J. P. *Nat. Rev. Drug. Discovery* **2009**, *8*, 69–85.
(23) National Committee for Clinical Laboratory Standards. Reference method for broth dilution antifungal susceptibility testing of yeast, 2nd ed.; Approved standard M27-A2; National Committee for Clinical Laboratory Standards, Wayne, PA, 2002.

NP8007649